

# Conceptual Design along with Mechanical Analysis of Neural Microelectrode

Hossein Amiri<sup>1</sup>, Reza Nadafi<sup>2,\*</sup>

<sup>1</sup> Department of Medical Physics and Biomedical Engineering, School of Medicine, Tehran University of Medical Sciences, Tehran, Iran

<sup>2</sup> Department of Mechanical Engineering, Amirkabir University of Technology, Tehran, Iran

Received: 13 July 2019

Accepted: 04 August 2019

DOI: <https://doi.org/10.18502/ftb.v6i3.1695>

<http://FBT.tums.ac.ir>

## Keywords:

Micro Electro Mechanical System;

Brain-Computer Interference;

Neural Microelectrode.

## Abstract

**Purpose:** Several studies were carried out in the field of neural microelectrode that caused the different generation of neural electrode appeared. Neural microelectrode has an important effect on the BCI interference and also is used in medical applications such as the detection and treatment process of different diseased. Therefore, achieving the structure of the electrode that has the high ability at recording and stimulating is so essential. This article aims at studying the different structure of Microelectrode, according to MEMS technology, and comparing their properties.

**Materials and Methods:** In this research, we introduce 7 designs for microelectrode fabrication that 3 designs are according to research that has been carried out so far and 4 designs have been proposed by authors and their fabricated process described. The microelectrode performance was determined by cost, biocompatibility, mechanical and electrical properties.

**Results:** The mechanical analysis was carried out using software and displacement, stress, and critical load factor calculated.

**Conclusion:** At last, the performance of the designed electrode was compared according to those parameters and the application of each design on the practical experiment described.

## 1. Introduction

The neural microelectrode is the interface between the physiological system and machine that enhances the possibility of contact and study organ activity. Studying tissue activity is a significant factor in medical applications such as detection and cures of the various diseases including epilepsy, functional brain disorders, and sleep disorder.

For example, in the cure, the process at epilepsy disease, we have two main choices, including using Magnetic Resonance Imaging (MRI) or deep neural electrode. The neural electrode has high accuracy in comparison to other methods. This advantage makes in a significant reduction in post-surgical complications that

it's due to the reduction of the volume of tissue removed from the brain. Several studies have been carried out for evaluating neural electrode properties. For example in [1-3] the fabrication process of microelectrode is introduced and the clinical result of using the electrode is shown.

In [4] a complete research was carried out for studying the Biocompatibility of composite material in human tissue and at results shown that polyimide material is the best composite for the medical implant at [5] Comparative mechanical analysis for one-dimensional microelectrodes that have different base geometry and layer thickness carried out. It's shown that the ratio of shaft length to base must not be so much or less that makes failing microelectrode in the insertion process.

### \*Corresponding Author:

Reza Nadafi, PhD

Department of Mechanical Engineering, Amirkabir University of Technology, Tehran, Iran

Tel: (+98) 915 1255645

Email: [rezanadafi@aut.ac.ir](mailto:rezanadafi@aut.ac.ir)

Also, according to the results, the sequence of mechanical resistance for a different material that is usually used in microelectrode fabrication from high to low are silicon, nickel, copper, and polyimide.

According to significant neural microelectrode in the medical applications, it's important to fabricate a proper electrode for different application. As mentioned before, the proper material and geometry was described but until now no comparative research has been carried out about the sequence of the fabricated process. The main aim of this article is to introduce a fabricated process with mechanical analysis using COMSOL Multiphasic software. Also, it provides appropriate microelectrode design path for new MEMS designer.

## 2. Materials and Methods

In this section, the basic concept of microelectrode performance and electrode geometry are shown. Also, the fabricated process of 7 designs and simulation software are described.

### 2.1. Performance of Neural Microelectrode

As mentioned above neural electrode is the interference between physiological tissue and electrical system. The electrical system current is the electron while in the physiological system current flow is chemical. Therefore the connection between these two systems required the interference that converts electrical to chemical current. The microelectrode does this conversion at the Chemical reaction of oxidation and reduction that is shown in Figure.1.

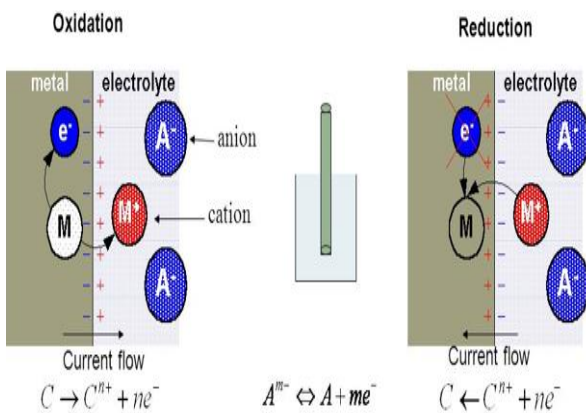


Figure 1. Oxidation and reduction reaction

### 2.2. Microelectrode Design

In this article, all studies performed on the one-dimensional microelectrode that has 4 sites on its shaft. The geometry of microelectrode used at the fabricated process is shown in the Figure 2.

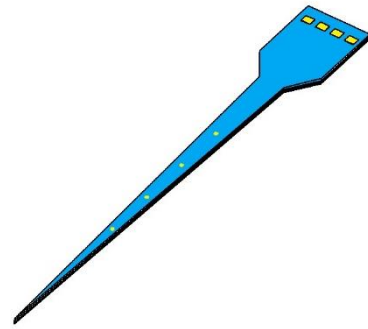


Figure 2. Geometry of the microelectrode

In this section, we introduce different designs for microelectrode fabrication according to MEMS technology.

#### 2.2.1. Design A

The global structure of this design is according to [6], that we changed materials of layer for a specific aim. The fabricated process contains 15 steps that the final structure of this design is shown in Figure.3.

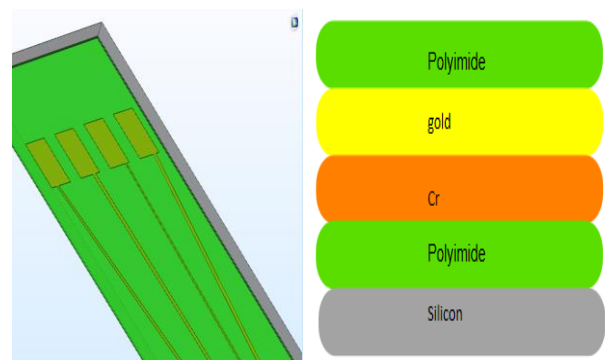


Figure 3. Structure of design A [6]

The steps of the fabricated process are as follows:

1. Choosing silicon as a substrate with a thickness above 70-micrometers.
2. Polishing a wafer surface to achieve a soft surface with 70-micrometer thickness.

3. Coating 5-micrometer polyimide on the silicon substrate.
4. Photoresist spin coating on the wafer.
5. Making the wiring pattern of the electrode that connects the site to pad, on the photoresist using direct masking method and UV radiation.
6. Putting the wafer in the diluted acid to remove the radiated part of the wafer.
7. Chrome deposition with 100-nanometer thickness, by using Chemical Vapor Deposition (CVD).
8. Au deposition with 100-nanometer thickness, by using chemical vapor deposition.
9. Photoresist etching. (Si wafer was put into a nitric acid solution)
10. Polyimide deposition with 5-micrometer thickness, by using the coating method.
11. Photoresist deposition, by using the coating method.
12. Putting the mask with a pattern for pad and site location on the photoresist then UV radiated.
13. Wafer was put into a diluted nitric acid solution to remove the irradiated layer
14. Etch process to open site and pad window.
15. Extract geometry designed for the electrode that is shown in Figure.1.

### 2.2.2. Design B

The global structure of this design is according to [7-9], that we changed materials of layer for a specific aim. The fabricated process contains 16 steps that the final structure of this design is shown in Figure.4.

The first 3 steps of the fabricated process are similar to design A and other steps are as follows:

4. Chrome deposition with 100-nanometer thickness, by using chemical vapor deposition.
5. Photoresist spin coating on the wafer.

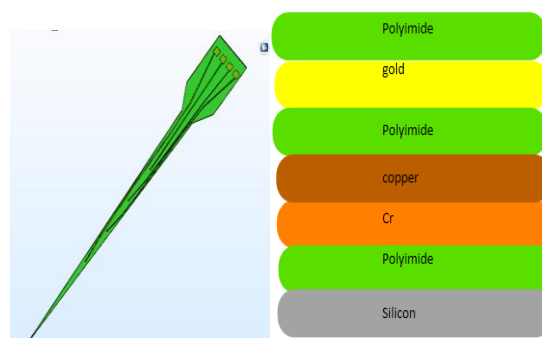


**Figure 4.** Structure of design B [7-9]

6. Making the wiring pattern of the electrode that connects the site to pad, on the photoresist using direct masking method and UV radiation.
7. Wafer was put into a diluted acid to remove the radiated part of the wafer.
8. Copper deposition with 700-nanometer thickness, by using Chemical Vapor Deposition (CVD).
9. Putting Silicon wafer into nitric acid solution in order to etch photoresist layer
10. Polyimide deposition with 5-micrometer thickness, by using the coating method.
11. Photoresist deposition, by using the coating method.
12. Putting masks with pad and site window on the photoresist then UV radiated.
13. Wafer was put into a diluted nitric acid solution to remove the irradiated layer.
14. Au deposition with 100-nanometer thickness, by using chemical vapor deposition.
15. Photoresist etching.
16. Extracting geometry designed from the electrode.

### 2.2.3. Design C

This design is suggested by the authors. The electrode was fabricated in 16 steps that enhances the biocompatibility of design A. The fabricated process is similar to design A but after 14 steps, the wafer is reversed and the polyimide with 3.2-micrometer thickness deposited. At the final step electrode shape is

extracted from the wafer. The final structure of this design is shown in Figure 5.

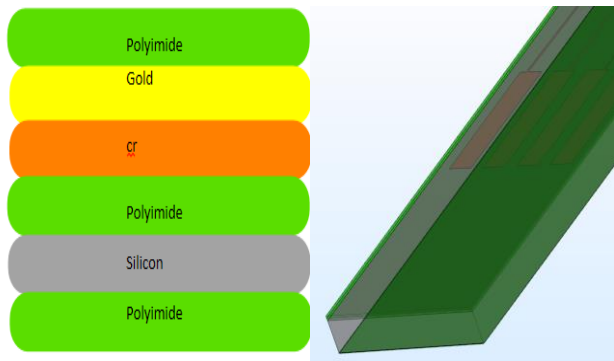


Figure 5. Structure of design C

### 2.2.4. Design D

This design is according to [4, 5, 10] that use less than the sacrifice layer. The fabricated process contains 15 steps that the final structure of this design is shown in Figure 6.

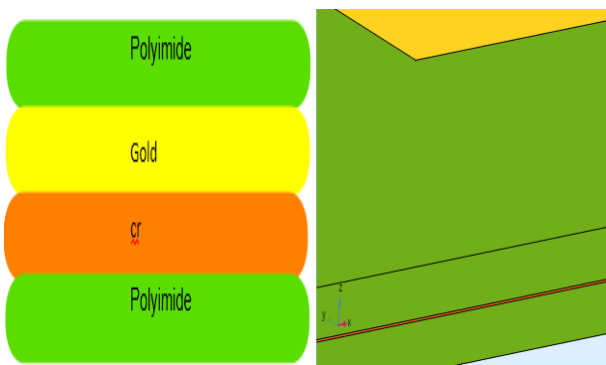


Figure 6. Structure of design D [4, 5, 10]

The steps for the fabricated process are as follows:

1. Choosing silicon as a substrate with a thickness above 50 micrometers.
2. Polishing a wafer surface to achieve a soft surface with 50-micrometer thickness.
3. Growing with the 0.5-micrometer thickness on the silicon substrate
4. Coating 15-micrometer polyimide on the wafer.
5. Photoresist spin coating on the wafer.

6. Making the wiring pattern of the electrode that connects the site to pad, on the photoresist using direct masking method and UV radiation.

7. Putting the wafer in the diluted acid to remove the radiated part of the wafer.

8. Chrome deposition with 700-nanometer thickness, by using Chemical Vapor Deposition (CVD).

9. Au deposition with 100-nanometer thickness, by using chemical vapor deposition.

10. Photoresist etching. (Si wafer was put into a nitric acid solution)

11. Polyimide deposition with 15-micrometer thickness, by using the coating method.

12. Photoresist deposition, by using the coating method.

13. Putting the mask with a pattern for pad and site location on the photoresist then UV radiated.

14. Putting wafer into a diluted nitric acid solution to remove the irradiated layer.

15. Etch processing to open site and pad window.

16. Putting wafer into a buffered hydrofluoric acid bath to remove the sacrifice layer.

17. Extracting geometry designed for the electrode that was mentioned in Figure 6.

### 2.2.5. Design E

This design was proposed by the authors that its structure is shown in Figure 7.

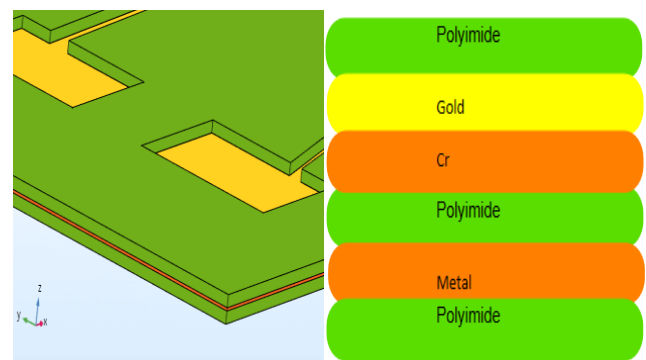


Figure 7. Structure of design E

The first 4 steps of the fabricated process are similar to design D and other steps are as follows:

5. Chrome deposition with 700-nanometer thickness, by using Chemical Vapor Deposition (CVD).

6. Coating 5-micrometer polyimide on the wafer.

7. Photoresist spin coating on the wafer.

8. Making the wiring pattern of the electrode that connects the site to pad, on the photoresist using direct masking method and UV radiation.

9. Putting the wafer in the diluted acid to remove the radiated part of the wafer.

10. Chrome deposition with 700-nanometer thickness, by using Chemical Vapor Deposition (CVD).

11. Au deposition with 100-nanometer thickness, by using chemical vapor deposition.

12. Photoresist etching. (Si wafer was put into a nitric acid solution)

13. Polyimide deposition with 15-micrometer thickness, by using the coating method.

14. Photoresist deposition, by using the coating method.

15. Putting the mask with a pattern for pad and site location on the photoresist then UV radiated.

16. Putting wafer into a diluted nitric acid solution to remove the irradiated layer.

17. Etch processing to open site and pad window.

18. Putting wafer into a buffered hydrofluoric acid bath to remove the sacrifice layer.

19. Extracting geometry designed for the electrode.

### 2.2.6. Design F

This design was proposed by the authors that its structure is shown in Figure 8.

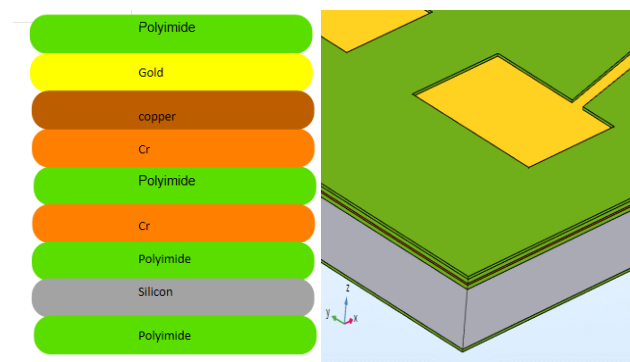


**Figure 8.** Structure of design F

The steps for the fabricated process are as follows:

1. Choosing silicon as a substrate with a thickness above 70-micrometers.

2. Polishing a wafer surface to achieve a soft surface with 70-micrometer thickness.

3. Coating 5-micrometer polyimide on the silicon substrate.

4. Chrome deposition with 500-nanometer thickness, by using chemical vapor deposition.

5. Coating 5-micrometer polyimide on the wafer.

6. Photoresist spin coating on the wafer.

7. Making the wiring pattern of the electrode that connects the site to pad, on the photoresist using direct masking method and UV radiation.

8. Putting the wafer in the diluted acid to remove the radiated part of the wafer.

9. Chrome deposition with 100-nanometer thickness, by using Chemical Vapor Deposition (CVD).

10. Copper deposition with 700-nanometer thickness, by using chemical vapor deposition.

11. Photoresist etching. (Si wafer was put into a nitric acid solution)

12. Polyimide deposition with 3.2-micrometer thickness, by using the coating method.

13. Photoresist deposition, by using the coating method.

14. Putting the mask with a pattern for pad and site location on the photoresist then UV radiated.

15. Putting wafer into a diluted nitric acid solution to remove the irradiated layer

16. Au deposition with 100-nanometer thickness, by using chemical vapor deposition.

17. Photoresist etching. (Si wafer was put into a nitric acid solution).

18. Wafer is reversed and 3.2-micrometer polyimide deposited.

19. Extracting geometry designed from the electrode.

6. Putting the wafer in the diluted acid to remove the radiated part of the wafer.

7. Chrome deposition with 100-nanometer thickness, by using chemical vapor deposition (CVD).

8. Copper deposition with 700-nanometer thickness, by using chemical vapor deposition.

9. Photoresist etching. (Si wafer was put into a nitric acid solution)

10. Polyimide deposition with 5-micrometer thickness, by using the coating method.

11. Photoresist deposition, by using the coating method.

12. Putting the mask with a pattern for pad and site location on the photoresist then UV radiated.

13. Putting wafer into a diluted nitric acid solution to remove the irradiated layer.

14. Au deposition with 100-nanometer thickness, by using chemical vapor deposition.

15. Photoresist etching. (Si wafer was put into a nitric acid solution)

16. Wafer is reversed and 3.2-micrometer polyimide deposited.

17. Extracting geometry designed from the electrode.

### 2.2.7. Design G

This design was proposed by the authors and the fabricated process has 18 steps. The final structure is shown in Figure 9.

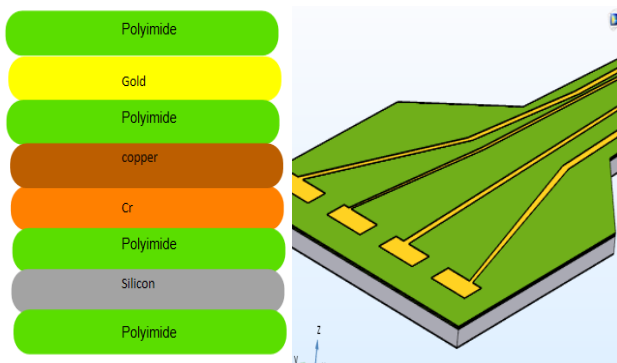


**Figure 9.** Structure of design G

The steps for the fabricated process are as follows:

1. Choosing silicon as a substrate with a thickness above 70 micrometers.

2. Polishing a wafer surface to achieve a soft surface with 70-micrometer thickness.

3. Coating 5-micrometer polyimide on the silicon substrate.

4. Photoresist spin coating on the wafer.

5. Making the wiring pattern of the electrode that connects the site to pad, on the photoresist using direct masking method and UV radiation.

### 2.3. Simulated Software

The mechanical analysis of all design is carried out by COMSOL Multiphasic.

### 3. Results

In this section, the results of the mechanical analysis for each design are shown. In our mechanical analysis, the solid mechanical physics was selected and we assumed that the insertion force at x, y-direction are equal and the base position of the electrode be fixed. According to the [11], the magnitude of the insertion force for the mice at each direction assumed 2.5mN. At last buckling analysis was carried out using the finite element method.

### 3.1.Design A

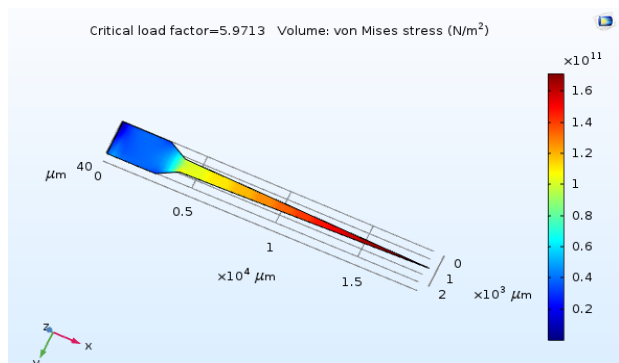


Figure 10. Stress of design A

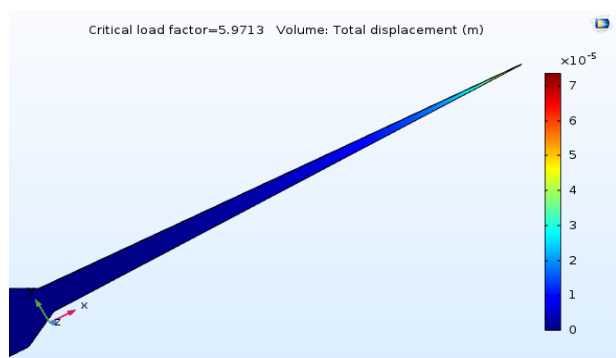


Figure 11. Displacement of design A

As shown in Figures 10, 11, the critical load factor is 5.9 and maximum displacement and stress happen at the tip of the electrode.

### 3.2.Design B

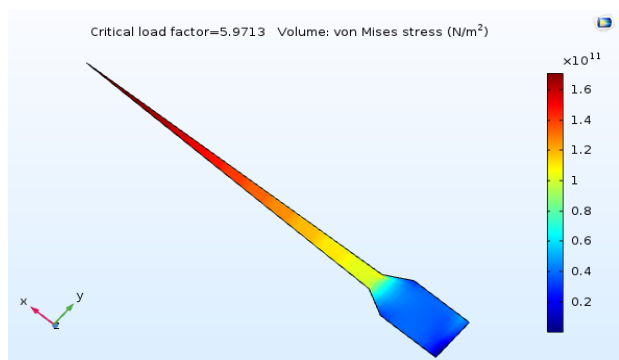


Figure 12. Stress of design B

As shown in Figures 12, 13, the critical load factor and stress is the same as the first (A) design. The maximum displacement is less than 70-micrometer.

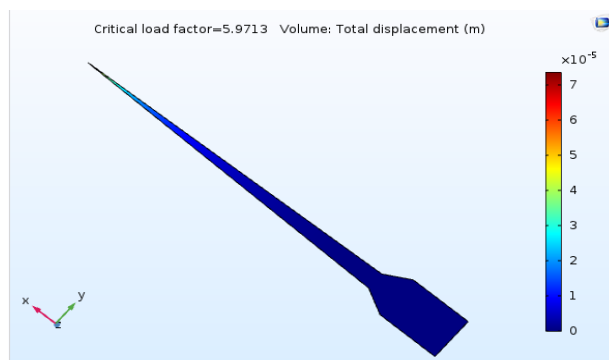


Figure 13. Displacement of design B

### 3.3.Design C

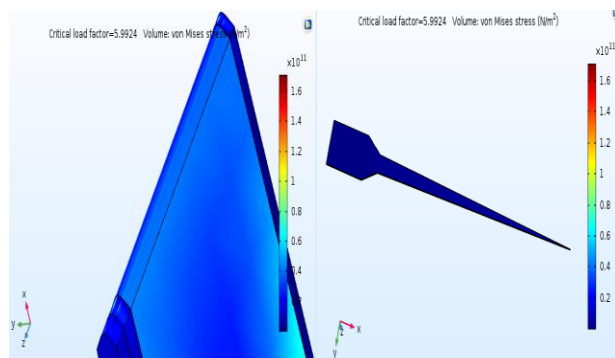


Figure 14. Stress of design C

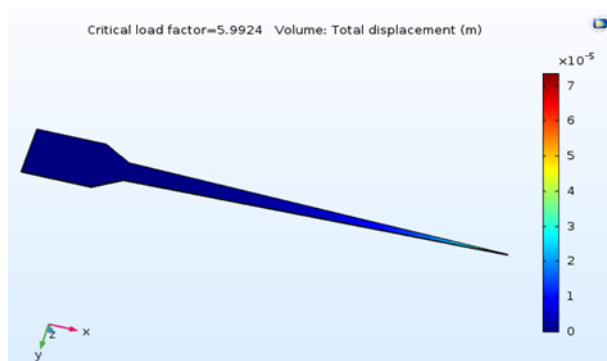


Figure 15. Displacement of design C

As shown in Figures 14, 15, the critical load factor is 5.99 and maximum stress happen at the silicon layer. The maximum displacement is less than 70-micrometer.

### Design D

As shown in Figures 16, 17, the critical load factor is 0.011 and maximum stress happen at Chrome layer. The maximum displacement is less than 2.2-millimeter.

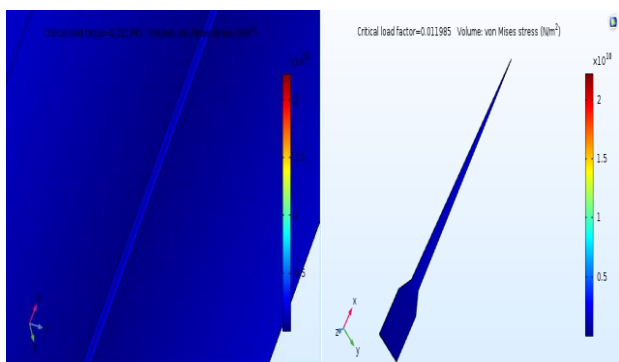


Figure 16. Stress of design D



Figure 17. Displacement of design D

### 3.4.Design E

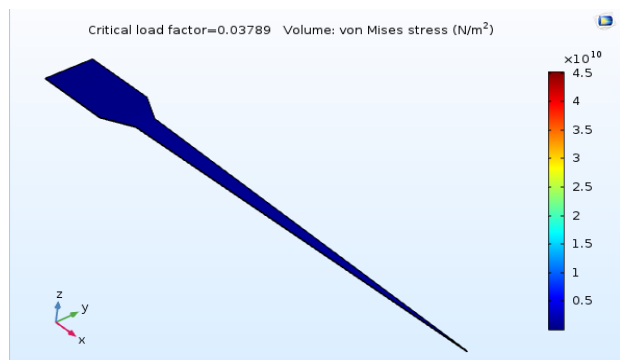


Figure 18. Stress of design E

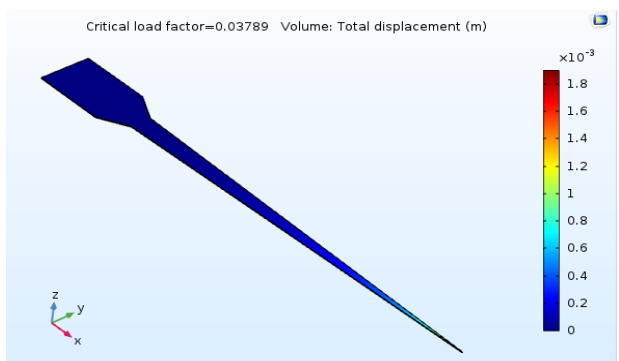


Figure 19. Displacement of design E

As shown in Figures 18, 19, the critical load factor is 0.037 and maximum stress happen at Chrome layer. The maximum displacement is less than 1.8-millimeter.

### 3.5.Design F

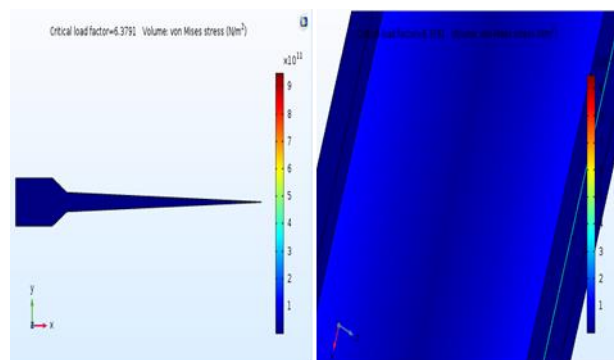


Figure 20. Stress of design F

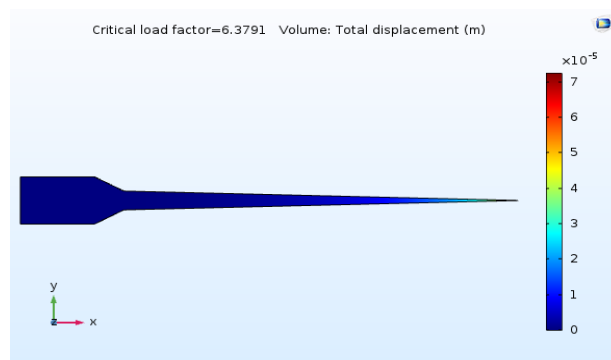


Figure 21. Displacement of design F

As shown in Figures 20, 21, the critical load factor is 6.37 and maximum stress happen at Chrome and silicon layers. The maximum displacement is less than 70-micrometer.

### Design G

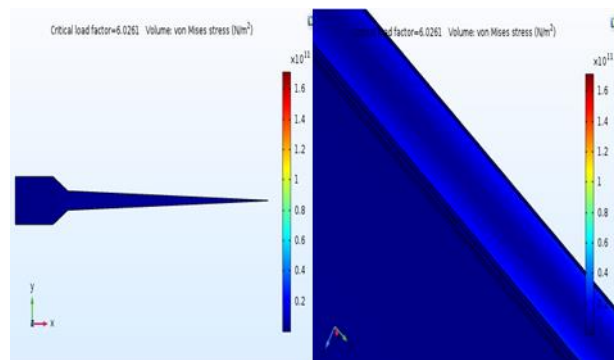
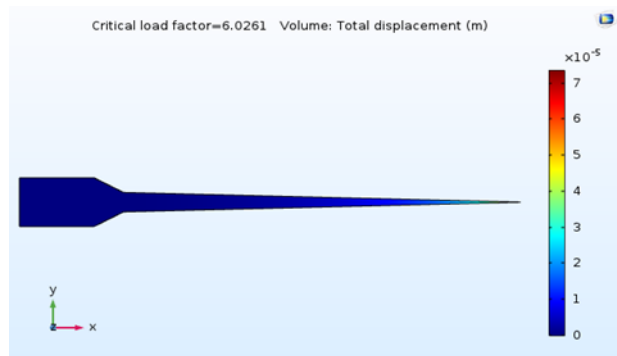


Figure 22. Stress of design G

As shown in Figures 22, 23, the critical load factor is 6.02 and maximum stress happen at the silicon layer. The maximum displacement is less than 70-micrometer.



**Figure 21.** Displacement of design G

## 4. Conclusion

In this article, we introduced 7 designs for the microelectrode fabrication process and their mechanical analysis provided in the previous section. According to research [1-4], the main properties of microelectrode that must be considered in the fabricated process are biocompatibility, cost, mechanic and electrical resistance.

In Table. 1, some properties of the designed electrode are sorted. The first 3 columns (i.e.: displacement, von miss stress, and critical load factor) are due to mechanical properties and steps with also the material of fabrication process determined the cost. Also, the material that connects the site to the pad and their dimension determined the electrical properties.

**Table 1.** Comparison of some properties of all designs

	Max. disp (um)	Max.stress (10 <sup>11</sup> *N/m <sup>2</sup> )	Critical Load Factor	Steps	Wiring Material
A	70	1.6	5.9713	15	Au
B	70	1.6	5.9713	16	Cu
C	70	1.2	5.9924	16	Au
D	2200	0.2	0.011	17	Au
E	1800	0.45	0.037	19	Au
F	70	9	6.37	19	Cu
G	70	1.6	6.02	17	Cu

The biocompatibility of the electrode depends on 3 factors that arise from acute and chronic tissue response

to the inserted electrode. The first factor is the amount of damage to the tissue at the insertion process. This damage increases as the thickness of the electrode increases. The second factor is tissue reaction to the electrode as foreign material that according to the research [1], polyimide and Au is the best material for this purpose. The third factor related to the flexibility of the electrode is that how much this flexibility increases, the amount of the neuron damaged in the insertion process decreases. Therefore, the quality of the signal received using the electrode is improved.

According to the result section and Table.1, each of the designed electrodes is used for a specific aim. The main feature of first (A) design is its lowest fabrication process cost, also it has good mechanical and electrical properties but its biocompatibility is bad. The electrical properties of the second (B) design is better than A, but its cost a little higher and other properties are approximately the same as A. The third design's biocompatibility in comparison to A and B designs is improved, but the other feature is the same as B. The fourth (D) design has the best biocompatibility while it has the worst mechanical resistance. Also, its cost is high and electrical properties are good. The mechanical resistance of fifth (E) design is better than D, but its cost is a little higher and other properties are approximately the same as D. The sixth (F) design has the highest cost and its biocompatibility is worse than C, but the mechanical and electrical features are at the highest level. The seventh (G) design has the same electrical properties as F and the biocompatibility and costs are a little higher, but mechanical resistance is decreased.

Therefore, the first (A) design is the best suggestion for the economical project and after that B and C are good, while designs D and E are suitable for the clinical project that subject safety is a more important factor. The F and G designs are proper structures in the case that the subject tissue is hard and mechanical resistance must be high to avoid failing in the insertion process.

## 5. Acknowledgment

This research development has been supported according to Contract 3514 by Cognitive Sciences & Technology Council of Iran.

## References

- 1- P. Fattahi, G. Yang, G. Kim, and M. R. Abidian, "A review of organic and inorganic biomaterials for neural interfaces," *Advanced materials*, vol. 26, no. 12, pp. 1846-1885, 2014.
- 2- H. Draz, S. Gabran, M. Basha, H. Mostafa, M. F. Abu-Elyazeed, and A. Zaki, "Comparative mechanical analysis of deep brain stimulation electrodes," *Biomedical engineering online*, vol. 17, no. 1, pp. 1-14, 2018.
- 3- N. Manam *et al.*, "Study of corrosion in biocompatible metals for implants: A review," *Journal of Alloys and Compounds*, vol. 701, pp. 698-715, 2017.
- 4- P. J. Rousche, D. S. Pellinen, D. P. Pivin, J. C. Williams, R. J. Vetter, and D. R. Kipke, "Flexible polyimide-based intracortical electrode arrays with bioactive capability," *IEEE Transactions on biomedical engineering*, vol. 48, no. 3, pp. 361-371, 2001.
- 5- A. L. Owens, T. J. Denison, H. Versnel, M. Rebbert, M. Peckerar, and S. A. Shamma, "Multi-electrode array for measuring evoked potentials from surface of ferret primary auditory cortex," *Journal of neuroscience methods*, vol. 58, no. 1-2, pp. 209-220, 1995.
- 6- K. A. Moxon, S. C. Leiser, G. A. Gerhardt, K. A. Barbee, and J. K. Chapin, "Ceramic-based multisite electrode arrays for chronic single-neuron recording," *IEEE Transactions on biomedical engineering*, vol. 51, no. 4, pp. 647-656, 2004.
- 7- R. J. Vetter, J. C. Williams, J. F. Hetke, E. A. Nunamaker, and D. R. Kipke, "Chronic neural recording using silicon-substrate microelectrode arrays implanted in cerebral cortex," *IEEE transactions on biomedical engineering*, vol. 51, no. 6, pp. 896-904, 2004.
- 8- D. R. Kipke, R. J. Vetter, J. C. Williams, and J. F. Hetke, "Silicon-substrate intracortical microelectrode arrays for long-term recording of neuronal spike activity in cerebral cortex," *IEEE transactions on neural systems and rehabilitation engineering*, vol. 11, no. 2, pp. 151-155, 2003.
- 9- K. Najafi, K. Wise, and T. Mochizuki, "A high-yield IC-compatible multichannel recording array," *IEEE Transactions on Electron Devices*, vol. 32, no. 7, pp. 1206-1211, 1985.
- 10- S. A. Boppart, B. C. Wheeler, and C. S. Wallace, "A flexible perforated microelectrode array for extended neural recordings," *IEEE Transactions on biomedical engineering*, vol. 39, no. 1, pp. 37-42, 1992.
- 11- M. Salcman and M. J. Bak, "A new chronic recording intracortical microelectrode," *Medical and biological engineering*, vol. 14, no. 1, pp. 42-50, 1976.